

© 2019 Malik Obeidin

LOCAL PROPERTIES OF RANDOM LINK DIAGRAMS

BY

MALIK OBEIDIN

DISSERTATION

Submitted in partial fulfillment of the requirements
for the degree of Doctor of Philosophy in Mathematics
in the Graduate College of the
University of Illinois at Urbana-Champaign, 2019

Urbana, Illinois

Doctoral Committee:

Professor Christopher Leininger, Chair
Professor Nathan Dunfield, Director of Research
Professor Anil Hirani
Professor Patrick Allen

Abstract

We describe a model of random links based on random 4-valent maps, which can be sampled due to the work of Schaeffer. We will look at the relationship between the combinatorial information in the diagram and the hyperbolic volume. Specifically, we show that for random prime alternating diagrams, the expected hyperbolic volume is asymptotically linear in the number of crossings.

If we do not restrict to prime alternating diagrams, and instead randomize the over/under strand at each crossing, it is known due to work of Chapman that the resulting diagrams are generically composite, as any tangle — including ones which, when inserted into a diagram, force a link to be composite — occurs many times in a large link diagram with high probability. Using enumerations of Bernardi and Fusy, we prove an asymptotic formula for probability that a tangle occurs in a specific location in a random (not necessarily prime) link diagram.

To Margaret.

Acknowledgments

I cannot repay a fraction of the debt I owe to my adviser Nathan Dunfield, an incredible, insightful, and compassionate mentor. I really got lucky. Working with Nathan was a privilege I will remember fondly for the rest of my life, and without his guidance, mathematical or otherwise, I would have gone nowhere.

I want to extend my sincerest thanks to my dissertation committee members: Nathan Dunfield, Chris Leininger, Anil Hirani, and Patrick Allen, for helpful comments and corrections.

I seriously doubt anyone in history has ever been more supportive than my wife Margaret has been during my studies. She is more precious to me than any mathematics, any career, or just about anything at all. Your confidence in me, your optimism, your hard work have contributed an equal share to this dissertation as I did.

My life has been indelibly shaped by my parents. They raised my brothers and I with absolute love, and even though we aren't all medical doctors, our success and happiness show how great a family grounded with love and loyalty can be. Thank you so much to Mom, Dad, Farres, Rami, and Kinan.

Thank you to Paul and Jill. You really made Champaign-Urbana feel like home and family; I don't know how Margaret and I would have coped without all of your help, your love, and your advice. You are the best father-in-law and mother-in-law someone could ever ask for.

Of all the things I love about my time in Urbana, there's nothing better than the amazing people I met. My peers in low dimensional topology were a joy to be around and work with. I want to thank my wonderful friends Nima, Parivash, Claire, David, Joseph, and Xinghua for being so awesome in every possible way. I really hope our paths converge again someday.

It was my privilege to be partially supported by NSF grant DMS-1510204 and Campus Research Board grant RB15127 during my tenure as a research assistant. These times were invaluable to my research and my development as a mathematician.

Table of Contents

List of Symbols	vi
Chapter 1 Introduction	1
1.1 Outline	4
Chapter 2 Background	5
Chapter 3 A Model for Random Links	7
Chapter 4 Alternating Diagrams	13
4.1 Enumeration and Sampling	13
4.2 Numerical Experiments	23
Chapter 5 Coin Flip Diagrams	27
References	43

List of Symbols

$\Pr[E]$	The probability of an event E .
$\mathbb{E}[X]$	The expected value of a random variable X .
$\mathbb{E}[X \mid Y]$	The conditional expected value of random variable X given Y .
$\text{Var}[X]$	The variance of a random variable X .
$\text{Cov}[X, Y]$	The covariance between two random variables X and Y .
$O(f(n))$	The Big O order of growth of a function $f(n)$.
Vol_n	The hyperbolic volume of the exterior of a random link diagram in a given set of link diagrams.
v_3	The volume the ideal, regular hyperbolic tetrahedron.
v_8	The volume the ideal, regular hyperbolic octahedron.
$PQ(n)$	The set of diagrammatically prime 4-valent rooted planar maps with n vertices.
$\text{Alt}(n)$	The set of alternating, rooted link diagrams with n crossings.
$\text{PAlt}(n)$	The set of alternating, rooted, diagrammatically prime link diagrams with n crossings
CF	The set of rooted link diagrams with n crossings.
PCF	The set of rooted, diagrammatically prime link diagrams with n crossings.
$LQ(n)$	The set of labeled quadrangulations with n faces.
$\text{Emb}_i^T(D)$	Indicator function for whether T embeds around edge i in D .
$\text{Num}^T(D)$	The number of edges in D around which T embeds.
$d_{\text{face}}(F_1, F_2)$	The <i>face distance</i> between two faces in a given diagram.

CHAPTER 1

Introduction

Random knots and links have been studied through a variety of avenues — initially inspired by physical problems such as the knotting that occurs in bacterial DNA. Additionally, link exteriors form an important, classical family of 3-manifolds. Since the set of links is countably infinite, one way to select randomly from this set is to filter links by some kind of complexity, such that the number of links of any given complexity is finite. From there, we can sample uniformly among links of a given complexity, and see what happens as the complexity increases without bound — the choice of this complexity gives different models of random links, which can have different asymptotic behaviors.

Some previously studied models of random knots and links include the Petaluma model [1], random polygonal walks [2], random braids [3], and the Chebyshev billiard table model [4]. In this thesis, we will examine a model which samples uniformly from (rooted) link diagrams of a given number of crossings.

In fact, there are four related models which we will mention:

- (I) Random alternating link diagrams
- (II) Random coin flip link diagrams
- (III) Random prime alternating link diagrams
- (IV) Random prime coin flip link diagrams

These models are defined in Chapter 3.

The “pattern theorem” established by Chapman [5] shows that in all of these models, and models of random *knot* diagrams as well, that for a given tangle T , one can find many copies of T sitting inside in a large random diagram. More specifically, he shows that for any 2-component, prime, 4-tangle T , there are constants $N \geq 0$, $d < 1$, and $c < 0$, so that

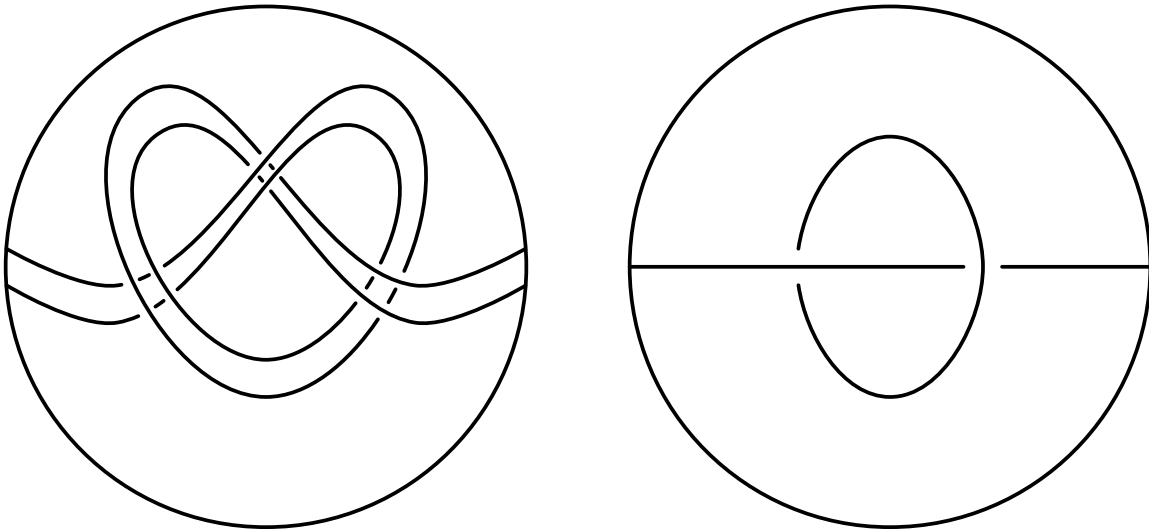


Figure 1.1

for a random diagram with $n \geq N$ crossings

$$\Pr[\text{a prime knot diagram } K \text{ contains } \leq cn \text{ copies of } T] < d^n$$

This occurs in other models as well — for example, for Gaussian random polygons [8]. The main interest here from the perspective of 3-dimensional topology and geometry is that generic link diagrams are *composite links*, hence non-hyperbolic. That is to say, there are “local” obstructions to hyperbolicity; for example, if either of the tangles in Figure 1.1 occur within a link diagram, the link diagram must represent a nonhyperbolic link (specifically, a satellite link). Surprisingly, this is not the case in the random braid model [3].

In exactly one of the four models above, link diagrams are generically hyperbolic: random alternating prime diagrams. Using the results of Lackenby, Thurston, and Agol in [6], we will show that the expected hyperbolic volume grows linearly in the number of crossings of the link diagram.

Theorem 1.1. *Let Vol_n be the random variable which returns the hyperbolic volume of a random alternating link diagram with n crossings. The expected hyperbolic volume is bounded by*

$$\left(\frac{19v_3}{54}\right)n + \left(\frac{10v_3}{27} - 2\right) + O\left(\frac{1}{n}\right) \leq \mathbb{E}[Vol_n] \leq v_8n$$

Numerically, the coefficients on n of the lower bound and upper bounds are approximately 0.3571 and 3.6638, respectively. The constants v_3 and v_8 are the volumes of the hyperbolic ideal regular tetrahedron and octahedron, respectively.

So, up to a term that goes to zero, the expected volume is bounded by (increasing) linear functions of the number of crossings. In big theta notation, $\mathbb{E}[Vol_n] = \Theta(n)$. The links we get in this model are generically hyperbolic — we also take the convention that the hyperbolic volume of a nonhyperbolic link is zero.

The bounds given in [6] are given in terms of the twist number of a diagram, not the crossing number. The main difficulty here is then the computation of the expected twist number in our model, which is in turn deduced from the expected number of bigons in the complement of the diagram. We only use the lower bound from [6] — it was pointed out to the author by Stavros Garoufalidis that there is an asymptotically sharp upper bound for the hyperbolic volume due to a construction of Dylan Thurston which divides the complement of an n -crossing link diagram in S^3 into n octahedra. Since the volume of such a hyperbolic octahedron is bounded by the volume of the ideal regular octahedron, we get an immediate linear upper bound of the volume as a function of the crossing number, and the bound on the expectation trivially follows [7].

In the widest class of link diagrams, where we do not restrict to alternating or prime diagrams, we compute an asymptotic formula for the probability of a given tangle occurring in a specific position with a random link diagram. The exact way we define a tangle diagram occurring in a link diagram is in Chapter 5. Roughly, we will work with *rooted* tangle diagrams, which have a specified oriented edge on the boundary circle, and such a diagram embeds in a link diagram if one can cut along a circle in the link diagram and obtain the tangle diagram.

Our formula shows that the probability a given tangle occurs depends only on the number of crossings in the tangle, and the number of boundary points.

Theorem 1.2. *Let T be a rooted, connected tangle diagram with n crossings and $2p$ boundary points, and let $Num^T(L)$ be the number of times T embeds in $L \in CF(N)$, a rooted link diagram with N crossings. Then,*

$$\mathbb{E}[Num^T] = \left(\frac{4P_{lim}(n, p)}{2^n} \right) N(1 + O(1/N))$$

where

$$P_{lim}(n, p) = \frac{3 \cdot 2^{(3p+1)} p^{\binom{3p}{p}}}{12^{(p+1+n)}}$$

Moreover, for any $\epsilon > 0$,

$$\Pr [Num^T < (1 - \epsilon)\mathbb{E}[Num^T] \text{ or } Num^T > (1 + \epsilon)\mathbb{E}[Num^T]] = O(1/N)$$

So, with high probability, Num^T is within any fixed fraction of its expectation for large N .

That is to say, in a large random link diagram, there will be around $P_{lim}(n, p) \cdot N$ occurrences of a tangle diagram with n crossings and $2p$ boundary points, where $P_{lim}(n, p)$ is given explicitly above. This says, for instance, that tangle diagrams with more boundary points will occur more often, assuming the same number of crossings. Also, each extra crossing in a tangle diagram decreases the expected number of occurrences by a factor of 12, for fixed p .

The fact that a given tangle will occur linearly often with high probability, as mentioned before, was already proved by Chapman. The main differences here with our proof are as follows:

- (I) We provide an explicit asymptotic formula for the expectation of this number of occurrences $\mathbb{E}[Num^T]$.
- (II) Along the way, we compute the probability that *around a specific edge*, a given tangle T embeds.
- (III) We show, in a specific sense defined in Chapter 5, that the correlation between the probabilities that a given tangle embeds around two random edges in a very large diagram goes to zero as the diagram becomes very large.

The above theorem provides a way of getting explicit lower bounds for additive invariants, i.e. link invariants that are additive under the connect-sum.

Corollary 1.3. *For a random link diagram in $CF(N)$, we have the following.*

- (I) *The Gromov invariant G : $\Pr[G < .000024N] = O(1/N)$*
- (II) *The log of the determinant $\log \det$: $\Pr[\log \det < .0003N] = O(1/N)$*
- (III) *The breadth of the Jones polynomial b_J : $\Pr[b_J < .0008N] = O(1/N)$*

So, there are explicit, linear lower bounds for these invariants which apply with high probability for large random link diagrams.

1.1 Outline

In Chapter 2, we give some background into the study of knots and their importance in three dimensional topology and geometry. In Chapter 3, we describe the model we are using and set up our notation. In Chapter 4, we show that the expected hyperbolic volume of a random alternating link in this model is linear in the number of crossings. We also present the results of numerical experiments about the behavior of the hyperbolic volume. In Chapter 5, we compute the probability of seeing a given tangle as a local picture in a generic random link diagram.

CHAPTER 2

Background

A *knot* is an embedding of a circle S^1 into the 3-sphere S^3 . Similarly, a *link with k components* is an embedding of the disjoint union of k circles $S^1 \sqcup \dots \sqcup S^1$ into S^3 . Typically, we will not distinguish between the image of this embedding and the embedding itself. The 3-sphere S^3 is homeomorphic to the one-point compactification of \mathbb{R}^3 , so links can be visualized as embedded in \mathbb{R}^3 instead. Knots and links are most often considered up to the equivalence of *ambient isotopy*; that is, two links are equivalent if there is an isotopy of S^3 taking one link to the other.

The most common way links are drawn is using a 2 dimensional projection, a *link diagram*. The complete definition for a link diagram we will use is in Chapter 3.

Links give rise to one of the most important classes of 3-manifolds, link exteriors. The *exterior* of a link L (also often called the *complement*) is the compact manifold obtained by taking an open regular neighborhood $N^\circ(L)$ and removing it from S^3 . In this thesis, we will suppress the open neighborhood, and denote the exterior $S^3 \setminus L$. The resulting manifold is a 3-manifold with boundary, whose boundary is the disjoint union of tori. Indeed, this class of manifolds can be used to obtain all orientable *closed* 3-manifolds, by attaching in solid tori $D^2 \times S^1$ along some choice of homeomorphisms of the boundary tori. This is the *Lickorish-Wallace Theorem*.

Due to the work of Thurston in the 1970's and 1980's [19], every link in S^3 comes in one of three types:

- (I) Torus links
- (II) Satellite links
- (III) Hyperbolic links

A *torus link* is one that is ambient isotopic to a link in the standard, unknotted torus in S^3 . A *satellite link* is a link whose exterior contains an *incompressible* torus which is not

boundary parallel. That is, there is a torus T embedded in the exterior of link L , so that every embedded disk D with $\partial D = D \cap T$ must intersect the link L , and T is not isotopic to a neighborhood of L . *Composite links* are examples of satellite links, made by taking a connect sum of two links L_1 and L_2 — that is, cutting L_1 and L_2 at some choice of points $p_1 \in L_1$ and $p_2 \in L_2$, and connecting the loose ends of L_1 with those of L_2 .

From the standpoint of the exteriors, the first two cases have exteriors with special surfaces — the work of Thurston showed that, in the absence of these special surfaces, the exterior must admit a *hyperbolic structure*. A *hyperbolic link* is one whose exterior admits a Riemannian metric of constant curvature -1 and finite volume. This fact is especially useful because such a metric for 3-manifolds is actually a topological invariant, by the Mostow rigidity theorem, so such links can be distinguished up to ambient isotopy by geometric quantities. One of the simplest, and most important quantities determined by a hyperbolic structure on a link complement is the volume.

In fact, Thurston wrote down specific equations, the *gluing equations*, to find a hyperbolic structure in terms of the shapes of ideal, hyperbolic tetrahedra. Starting with an ideal triangulation of a link exterior (or any 3-manifold with torus boundary), the system of equations can be numerically solved, and hence the hyperbolic volume is actually a readily computable invariant. This procedure was implemented by Weeks in the program *SnapPea*, which is a core component of the package *SnapPy* used in this thesis to compute the volumes of hyperbolic links [25].

In general, the case of hyperbolic manifolds is seen as a “generic” condition, the hardest and most general case to consider. Tables of knots, classified up to ambient isotopy, have been made up to 16 crossings by Hoste, Thistlethwaite, and Weeks; of these, 13 are torus knots, 20 are satellite knots, and the other roughly 1.7 million are all hyperbolic [10]. For this reason, one might conjecture that, up to ambient isotopy, probability of a random knot in some sense with n crossings being hyperbolic tends to 1 as n increases. However, this depends on how one defines “random knot”, as indicated in the introduction.

CHAPTER 3

A Model for Random Links

One natural way to randomly sample links is through link diagrams. A *rooted planar map* is an equivalence class of embeddings of a connected planar graph into the plane, where the equivalence is given by orientation-preserving homeomorphisms of the sphere, and where one oriented edge called the *root* is specified. The homeomorphism is also required to take root to root.

This extra choice of oriented edge is made because for a *rooted* planar map, there can be no nontrivial symmetries: if $D \subset S^2$ is (the image of) a planar map with root r , and $f : S^2 \rightarrow S^2$ is an orientation preserving homeomorphism with $f(D) = D$ and $f(r) = r$, then f maps *every* vertex, face, and oriented edge of D onto itself. See, for example, [14] for details. The lack of nontrivial symmetries make enumerations much simpler. We will also sometimes refer to the vertex at the “back” of the root as the *root vertex*, and the face on the right side of root as the *root face*.

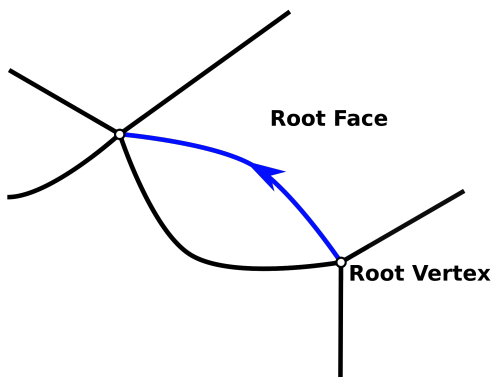


Figure 3.1: The root edge, face, and vertex of a planar map.

By “graph” above, we really mean multi-graph — loops and multiple edges are allowed. Note that a *4-valent* planar map (all vertices having valence 4) can be viewed as a projection

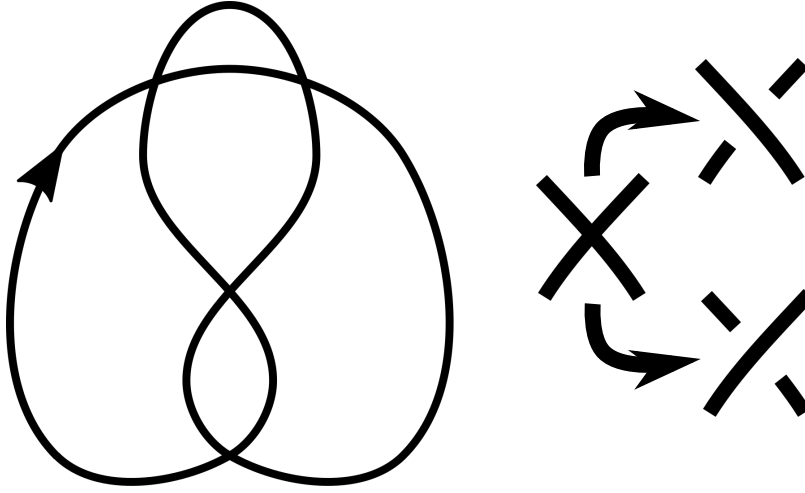


Figure 3.2: Left: An element of $Q(4)$. Right: the two possible choices at a vertex to resolve into a link diagram crossing.

of a link in \mathbb{R}^3 into the plane; to specify a link from a 4-valent planar map, we think of the vertices as crossings and specify which strand goes over which.

We will consider the set of all rooted 4-valent planar maps with n vertices, which we denote $Q(n)$. This set $Q(n)$ can be thought of as the set of link “shadows”, which is like a link diagram, but without the indication of which strand goes over which. To turn an element of $Q(n)$ into a link diagram, one makes a choice at each of the n vertices to turn them into crossings. See Figure 3.2.

Due to the work of Schaeffer, it is actually possible to sample *uniformly* at random from $Q(n)$; in fact, it can be done very quickly on a computer. Schaeffer implemented his algorithm in *planarmap* [12]. This software is used in *SnapPy* to generate random links with different properties.

From the point of view of knots and links, one potential issue with using $Q(n)$ to generate link diagrams is that many elements of $Q(n)$ are connect sums of simpler diagrams, no matter how we choose the crossings. Specifically, if there are two edges in the planar map which, when cut, disconnect the map, we say that map is *diagrammatically composite*. Otherwise, the map is *diagrammatically prime*. See Figure 3.3.

We’ll denote the set of diagrammatically prime 4-valent rooted planar maps with n vertices by $PQ(n)$. This case is also handled by Schaeffer in *planarmap*. Both classes had been enumerated with non-constructive generating function approaches. The set $Q(n)$, among other related sets, was enumerated by Tutte [14, 15], and $PQ(n)$ was enumerated by Brown [16], though in slightly disguised form. We explain the connection between $PQ(n)$ and

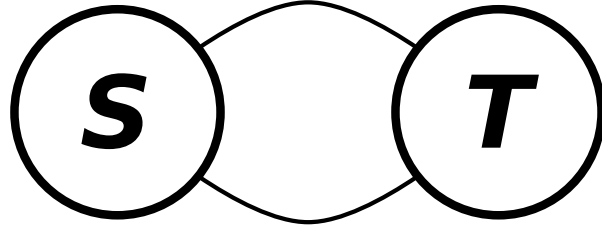


Figure 3.3: The schematic of a map which is not diagrammatically prime. Here, we can cut along two edges and disconnect the map.

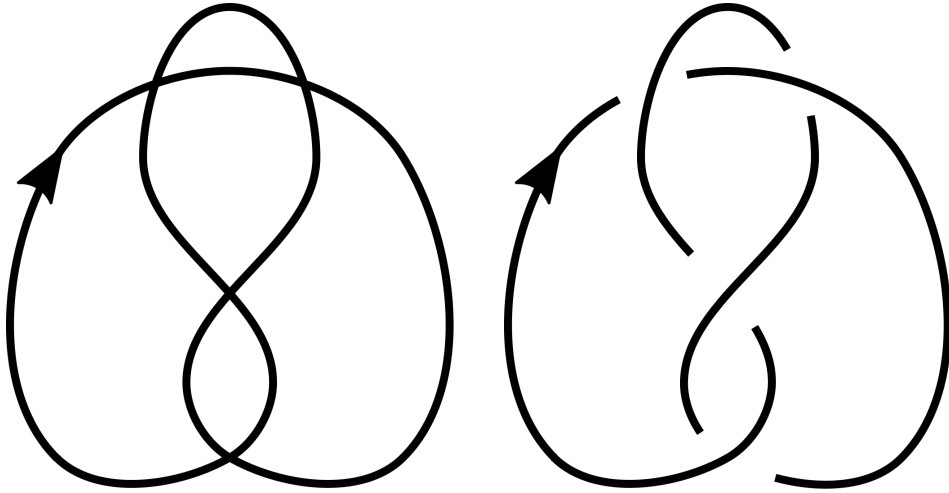


Figure 3.4: Alternating the crossings for the figure eight shadow.

Brown's *nonseparable planar maps with n edges* in the next section. The enumerations are

$$|Q(n)| = \frac{2(3^n)(2n)!}{n!(n+2)!}$$

$$|PQ(n)| = \frac{2(3n-3)!}{n!(2n-1)!}$$

For each of these, we will consider two different models of random link diagrams; one obtained by alternating the crossings, and one obtained by flipping a coin at each crossing. There are exactly two ways to make an element of $Q(n)$ or $PQ(n)$ into an alternating link diagram — however, the root allows us to fix one of these choices. Specifically, we stipulate that the root edge goes over-to-under, giving us a unique choice of alternating link diagram. See Figure 3.4.

However, we can also just flip a coin at each vertex of an element of $Q(n)$ or $PQ(n)$ to determine which strand is over and which is under; essentially, this is considering *all* link

diagrams with n crossings. So, there are four models of random links we consider:

- (I) $Alt(n) := \{\text{alternating, rooted link diagrams with } n \text{ crossings} \}$
- (II) $PAlt(n) := \{\text{alternating, rooted, diagrammatically prime link diagrams with } n \text{ crossings} \}$
- (III) $CF(n) := \{\text{rooted link diagrams with } n \text{ crossings} \}$
- (IV) $PCF(n) := \{\text{rooted, diagrammatically prime link diagrams with } n \text{ crossings} \}$

For each of these four, we have a method to sample uniformly; first sampling an element of $Q(n)$ or $PQ(n)$, and then either alternating or flipping a coin at each vertex. This gives immediately the enumerations

- (I) $|Alt(n)| = |Q(n)|$
- (II) $|PAlt(n)| = |PQ(n)|$
- (III) $|CF(n)| = 2^n |Q(n)|$
- (IV) $|PCF(n)| = 2^n |PQ(n)|$

For any knot or link diagram, the projection which forgets the crossing data, and returns an element of $Q(n)$ is called the *shadow* of the knot or link diagram.

We emphasize that just because a given link diagram is diagrammatically prime, it does not mean that the link itself is prime — only that it is not an “obvious” connect sum in that particular diagram for the link. Using *planarmap*, one can sample uniformly at random from $Q(n)$ and $PQ(n)$, and hence any of the four models above. See Figures 3.5 through 3.8 for examples generated from *SnapPy*.

As shown by Chapman in [5], $Q(n)$ and $PQ(n)$ are subject to a “pattern theorem”, which, informally, shows that a fixed tangle occurs inside of a very large random link diagram many times. More formally, a *2p-tangle shadow* is a planar map which has all vertices of degree 4 except for one vertex, called the *exterior vertex*, which can have any even degree $2p$. When drawing such a diagram, we will cut a small disk around the exterior vertex, leaving a disk which can be drawn in the standard way tangles are drawn.

For an oriented, embedded circle C in S^2 meeting $D \in Q(n)$ in exactly $2p$ non-vertex points, we can cut along this circle, and keep the left side, a $2p$ tangle shadow. Technically, we must first collapse the boundary circle, to once again obtain a planar map in S^2 . Then, for a link shadow $D \in Q(n)$ we say that a $2p$ -tangle shadow T *embeds in* D if there is such a circle C so that T is the tangle shadow resulting from cutting along C as above. We

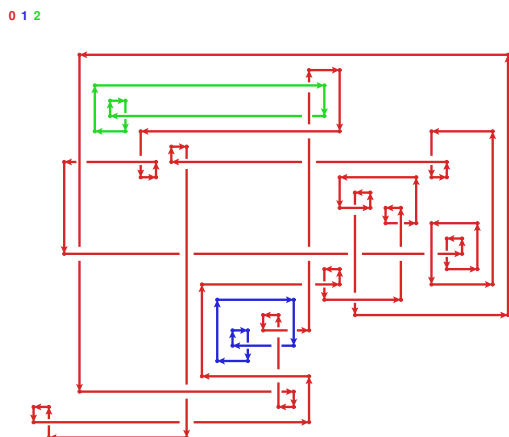


Figure 3.5: An element of $Alt(30)$

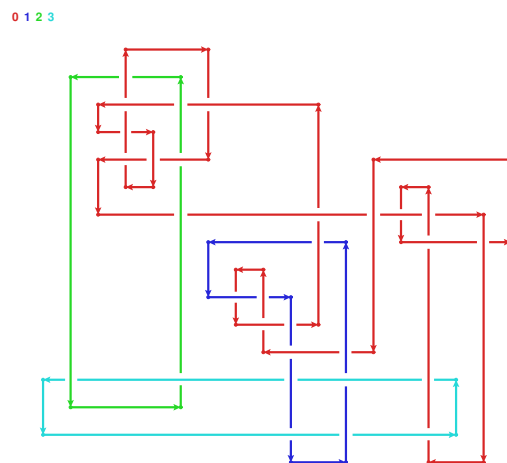


Figure 3.6: An element of $PAlt(30)$

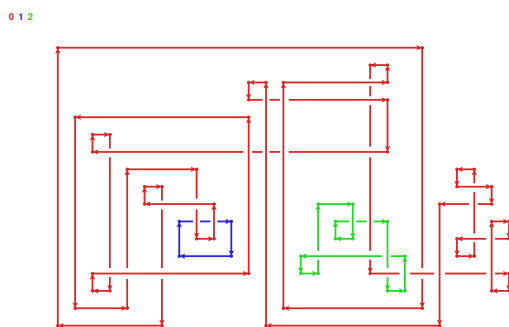


Figure 3.7: An element of $CF(30)$

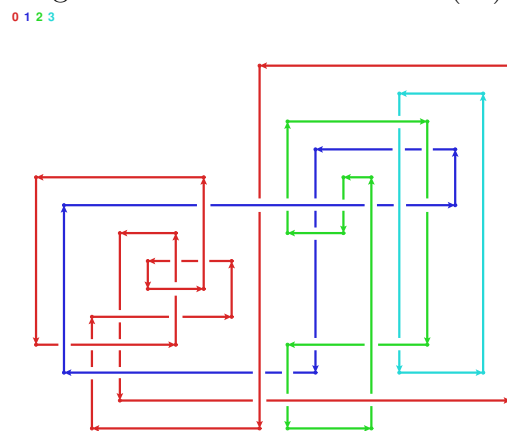


Figure 3.8: An element of $PCF(30)$

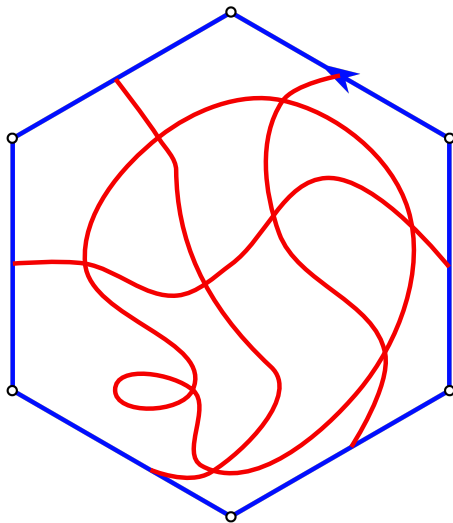


Figure 3.9: A tangle shadow cut along a topological circle from a larger link shadow.

will be interested in the *number of times T occurs in D* — that is, the number of oriented, embedded circles which, after cutting and collapsing, result in T . This count is considered up to ambient isotopy, fixing the sequence of edges that the circle C crosses. See Figure 3.9.

In [5], Chapman shows that for any T , the *probability* that T embeds in a random $D \in Q(n)$ goes to 1 as $n \rightarrow \infty$. In fact, he shows that for any T , in any of the classes above, as well as knot diagrams, there are constants $N \geq 0$, $c > 0$, and $d < 1$ so that

$$\Pr [T \text{ embeds } \leq cn \text{ times}] < d^n$$

In other words, the probability that there are fewer than “linearly many” copies of any given T in a random $D \in Q(n)$ is exponentially small.

This phenomenon forces three out of the four models described above to be nonhyperbolic — $Alt(n)$ and $CF(n)$ contain connect sums with any link, and $PAlt(n)$ contain “doubled” knots which force the link to be satellite. See Figure 1.1. The last case, $PAlt(n)$, is actually generically hyperbolic, and will be examined in the next chapter.

CHAPTER 4

Alternating Diagrams

4.1 Enumeration and Sampling

Various classes of planar maps were enumerated in a series of papers by Tutte and Brown [14, 15]. The class we are interested in was enumerated by Brown in [16], though in slightly disguised form. The maps enumerated are *nonseparable rooted planar maps with n edges* — planar maps without a loop or *cut-vertex*. A cut-vertex is a vertex V which partitions the edges of the map into two sets which only share V as a vertex. The set of nonseparable rooted planar maps with n edges is in bijection with $PQ(n)$ through the medial bijection (see Figure 4.1).

Note that a cut vertex corresponds exactly to a place where the corresponding link diagram (under the medial bijection) can be separated into two halves, connected by two strands. The convention to transfer the root to the 4-valent map is as in Figure 4.1. One should be careful above the inverse of the medial bijection — it appears that, around a vertex of a 4-valent map, there are four choices of oriented edge coming out, hence there should be four associated planar maps after applying the inverse. There appear to only be two, since we have two orientations of the edge that corresponds to that vertex in the planar map. However, there are two different (unrooted) planar maps that give the same (unrooted) 4-valent map after the medial bijection, a map and its dual, and each of these will have two rootings of a given edge. These four possibilities give the four rootings of the corresponding vertex after the medial bijection.

Jacquard and Schaeffer in [17] describe an algorithm to sample efficiently from $PQ(n)$, so we can sample from prime alternating link diagrams of size n . In our case, we wish to see that the volume indeed grows linearly in the size of the diagram, as one might expect from the following result from [6]:

Theorem 4.1 (Lackenby, Agol, Thurston 2004). *Let D be a prime, alternating diagram of*

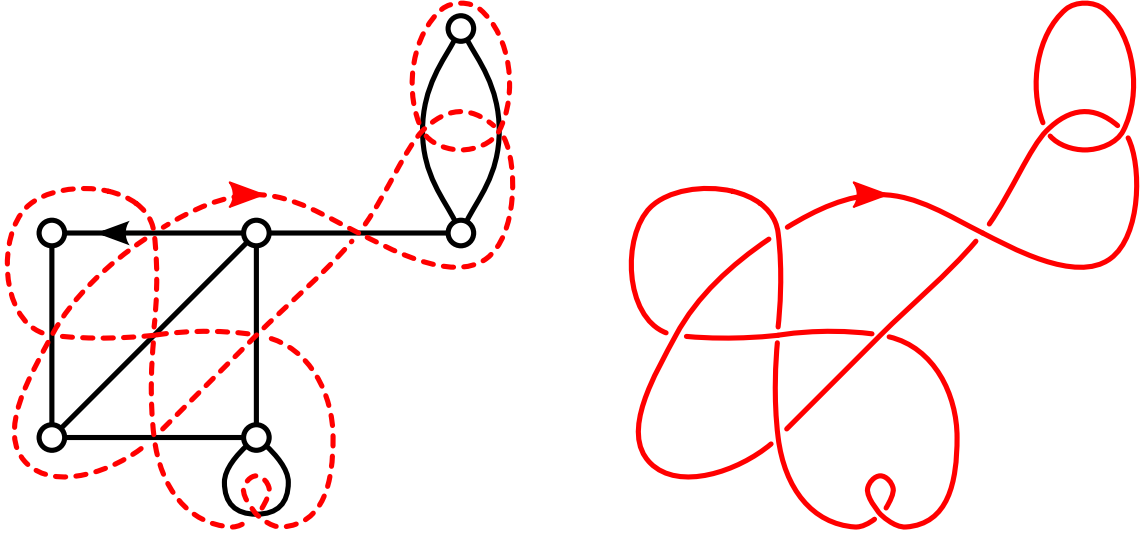


Figure 4.1: The medial bijection: to every planar map we can associate a 4-valent planar map by creating a vertex at the midpoint of each edge and connecting around each face. The root of the new map is taken by convention to be the outward edge 2nd from the original clockwise, as shown. The example here is *separable*: for example, the root vertex is a cut vertex. On the right, we have the resulting alternating link diagram.

a hyperbolic link K . Then

$$v_3(t(D) - 2)/2 \leq \text{Vol}(S^3 - K) < 10v_3(t(D) - 1) \quad (1)$$

where $v_3 \approx 1.01494$ is the volume of a regular hyperbolic ideal tetrahedron.

Moreover, the upper bound is asymptotically sharp.

Here $t(D)$ represents the *twist number* of a diagram, which is defined in [6] as the number of twist regions. A *twist region* is a maximal chains of bigons, arranged end to end, or a crossing not adjacent to any bigon. An example is given in Figure 4.2.

Note that for each bigon chain, the number of crossings is one more than the number of bigons. Since the twist regions partition the crossings and the bigons of D ,

$$\begin{aligned} t(D) &= \sum_{\text{twist regions } T} 1 \\ &= \sum_{\text{twist regions } T} [(\# \text{ crossings in } T) - (\# \text{ bigons in } T)] \\ &= (\# \text{ crossings in } D) - (\# \text{ bigons in } D) \end{aligned} \quad (2)$$

That is, the twist number of a diagram is simply the number of crossings minus the number

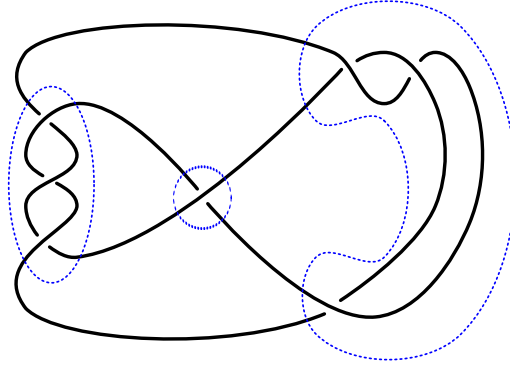


Figure 4.2: This diagram has the 3 twist regions outlined. Note that there are 7 crossings, and 4 bigons in the complement.

of bigons in the complement. There is one corner case here where the formula doesn't hold: if the bigon chain connects to itself to make a loop, we then have a connected component of the link diagram which is the standard diagram of the torus link $T(2, n)$. Since our diagram is assumed connected, there is only one such unrooted diagram to consider, which has two rootings in $PQ(n)$, as shown in Figure 4.3. In this case, the twist number $t(D)$ is just 1.

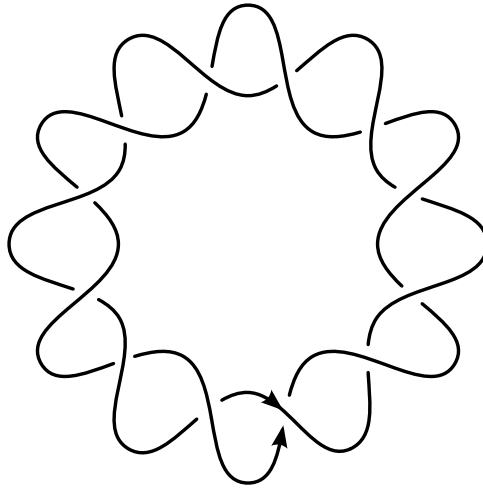


Figure 4.3: The torus link $T(2, 12)$. The root edge will either have a bigon to its right, or a larger face. Those two cases, after homeomorphism of the sphere, can be transformed to the two rootings shown above.

So, in order to get bounds on the expected volume in our model, we can simply find the expected number of bigons. It is Brown's enumeration that allows us to do this. We first find the probability that a randomly chosen element of $PQ(n)$ will have a bigon as its root *face*.

In the medial bijection between nonseparable planar maps and $PQ(n)$, a nonseparable planar map where the root vertex has valence m corresponds to an element of $PQ(n)$ where the root face has m sides. Let $PQ(n, m)$ be the subset of all elements of $PQ(n)$ where the root face has m sides. Then, we have the enumeration

Theorem 4.2 (Brown 1962). *The number of nonseparable planar maps with n edges and root valence m is given by:*

$$|PQ(n, m)| = \left(\frac{m}{(2n - m)!} \right) \sum_{j=m}^{\min(n, 2m)} \frac{(3m - 2j - 1)(2j - m)(j - 2)!(3n - j - m - 1)!}{(n - j)!(j - m)!(j - m + 1)!(2m - j)!}$$

where $n \geq m \geq 2$.

The number of nonseparable planar maps with n edges (and no other restriction) is

$$|PQ(n)| = \frac{2(3n - 3)!}{n!(2n - 1)!}$$

Since we select uniformly from all diagrams, the probability that the root face has size m is then given by

$$P(n, m) = \frac{|PQ(n, m)|}{|PQ(n)|}$$

We will use this to compute the expected number of m -gons in a diagram chosen in our model. Immediately, this gives us the following fact.

Lemma 4.3. *Let F_m be the random variable defined on $PQ(n)$ with the uniform probability given by*

$$F_m(D) = \begin{cases} 1/m & \text{if root face is size } m \\ 0 & \text{otherwise} \end{cases}$$

Then,

$$\mathbb{E}[F_m] = \frac{1}{m} \frac{|PQ(n, m)|}{|PQ(n)|} = \frac{1}{m} P(n, m)$$

In order to relate this to the number of m -gons in a diagram, we partition $PQ(n)$ into the equivalence classes of *unrooted* diagrams. That is, we group together all rooted diagrams which are different rootings of the same unrooted diagram. The useful and generic case here is when the underlying unrooted diagram has no nontrivial automorphisms — orientation preserving homeomorphisms of the sphere taking the diagram to itself which actually permute the edges. We call such diagrams *asymmetric*. Equivalently, a diagram is *asymmetric* if there are exactly $4n$ inequivalent rootings of the unrooted diagram, one for each oriented edge.

We denote the equivalence class of D under this equivalence relation by $[D]$, and the number of m -gons in D by $N_m(D)$.

To relate F_m to our desired N_m , we have the following simple lemma.

Lemma 4.4. *Let $D \in PQ(n)$ be asymmetric, and N_m and F_m as above. Then, the conditional expectation over the equivalence class $[D]$ is*

$$\mathbb{E}[F_m \mid [D]] = \frac{1}{4n} N_m(D)$$

Proof. If D is asymmetric, then we are computing the average over all rootings r of the underlying unrooted diagram, of which there are $4n$. Calling D_r the diagram in $[D]$ with root r , then we have

$$\mathbb{E}[F_m \mid [D]] = \frac{1}{4n} \sum_r F_m(D_r)$$

For each root r , if the root face (the face to the right of r) is not an m -gon, then we get zero. Otherwise, we get a contribution of $1/m$, which will occur for all m edges around that face. So, the sum gives $N_m(D)$, as desired. \square

In order to now get estimates on the expectation of N_m , we need to know that “most” diagrams are asymmetric. Fortunately, this is a well studied problem; in particular, it is known that the proportion of nonseparable planar maps which are symmetric is exponentially small [18]. With these facts, we can complete the computation of the expectation of N_m .

Theorem 4.5. *Let N_m be the random variable on $PQ(n)$ with the uniform probability measure defined as above. Then, the expectation of N_m is given by*

$$\mathbb{E}[N_m] = \frac{4n}{m} P(n, m) + O(na^n)$$

for some $a \in (0, 1)$.

Proof. Take representatives A_i , $i \in \{1, \dots, k\}$, of each of the equivalence classes of asymmetric diagrams. Then, by the law of total expectation, we can split the expectation of N_m as follows:

$$\mathbb{E}[N_m] = \sum_{i=1}^k \mathbb{E}[N_m \mid [A_i]] P([A_i]) + \mathbb{E}[N_m \mid S_n] P(S_n)$$

where S_n is the set of all symmetric diagrams in $PQ(n)$. The conditional expectation over the equivalence class $[A_i]$ of N_m is $N_m(A_i)$, as N_m is constant over the equivalence class,

since the number of m -gons depends only on the unrooted diagram. So, we have

$$\mathbb{E}[N_m] = \sum_{i=1}^k N_m(A_i)P([A_i]) + \mathbb{E}[N_m | S_n]P(S_n)$$

Substituting in with Lemma 4.4, we have

$$\mathbb{E}[N_m] = \sum_{i=1}^k (4n \cdot \mathbb{E}[F_m | [A_i]])P([A_i]) + \mathbb{E}[N_m | S_n]P(S_n) \quad (3)$$

Now, we turn to the expectation of F_m , which is known by Lemma 4.3 and related to N_m by Lemma 4.4. We decompose in the exact same way as with N_m :

$$\mathbb{E}[F_m] = \sum_{i=1}^k \mathbb{E}[F_m | [A_i]]P([A_i]) + \mathbb{E}[F_m | S_n]P(S_n)$$

Note that we get a similar term to before. Multiplying through by $4n$, and subtracting the rightmost term gives

$$4n \cdot \mathbb{E}[F_m] - 4n \cdot \mathbb{E}[F_m | S_n]P(S_n) = \sum_{i=1}^k 4n \cdot \mathbb{E}[F_m | [A_i]]P([A_i])$$

Now, we can substitute directly back into 3 above, and obtain

$$\mathbb{E}[N_m] = (4n \cdot \mathbb{E}[F_m]) - (4n \cdot \mathbb{E}[F_m | S_n]P(S_n)) + \mathbb{E}[N_m | S_n]P(S_n)$$

We know from [18] that the probability of selecting a symmetric diagram is exponentially small as $n \rightarrow \infty$, so $P(S_n) = O(a^n)$, $0 < a < 1$. The conditional expectation of F_m over S_n is bounded (at most 1), and the conditional expectation of N_m is at most linear in n , as the highest it can be is bounded by the total number of faces, which is $n + 2$ by a simple Euler characteristic argument. Hence, by Lemma 4.3 and these facts, we have the desired result of

$$\mathbb{E}[N_m] = \frac{4n}{m}P(n, m) + O(na^n)$$

□

So, to find explicitly the expected value of N_m , it remains to get a formula for $P(n, m)$. In fact, the only case we need, to compute the expected number of bigons, is $P(n, 2)$, which we can compute explicitly and directly from the definitions.

Lemma 4.6. *The limiting behavior of $P(n, 2)$ is given by*

$$P(n, 2) = \frac{4}{27} + \frac{10}{27n} + O\left(\frac{1}{n^2}\right)$$

Proof. By the enumeration of Brown in Theorem 4.2,

$$|PQ(n, 2)| = \frac{2}{(2n-2)!} \left(\frac{(3n-5)!}{(n-2)!} - 2 \frac{(3n-6)!}{(n-3)!} - 3 \frac{(3n-7)!}{(n-4)!} \right)$$

From here, we can factor out the factorials

$$|PQ(n, 2)| = \frac{2}{(2n-2)!} \frac{(3n-7)!}{(n-4)!} \left(\frac{(3n-5)(3n-6)}{(n-2)(n-3)} - 2 \frac{(3n-6)}{(n-3)} - 3 \right)$$

Dividing now by $|PQ(n)|$ and simplifying the right factor, we can pair all the factorials so that we are left with just a rational function in n

$$\frac{|PQ(n, 2)|}{|PQ(n)|} = \frac{(2n-1)(n)(n-1)(n-2)(n-3)}{(3n-3)(3n-4)(3n-5)(3n-6)} \left(\frac{6}{n-3} \right)$$

So simplifying and expanding the first two terms of the Laurent series about ∞ gives

$$P(n, 2) = \frac{4}{27} + \frac{10}{27n} + O\left(\frac{1}{n^2}\right)$$

which is the formula claimed. □

This gives the expected twist number of a diagram is $t(D) \approx (1 - 8/27)n = 19n/27$ for large n . For larger m , we can numerically approximate with large values for n the expected portion of m -gons.

m	$4/m \cdot P(1000, m)$
2	0.2964445
3	0.2415913
4	0.1643246
5	0.1068911
6	0.0686226
7	0.0439052

Now that we have asymptotics for the twist number, using the bounds in (1), we can get the asymptotic estimates on the expectation of the volume, and prove the first theorem of the introduction, repeated here.

Theorem 1.1. *Let Vol_n be the random variable which returns the hyperbolic volume of a random alternating link diagram with n crossings. The expected hyperbolic volume is bounded by*

$$\left(\frac{19v_3}{54}\right)n + \left(\frac{10v_3}{27} - 2\right) + O\left(\frac{1}{n}\right) \leq \mathbb{E}[Vol_n] < \left(\frac{190v_3}{27}\right)n + \left(\frac{200v_3}{27} - 1\right) + O\left(\frac{1}{n}\right)$$

Numerically, the coefficients on n of the lower bound and upper bounds are approximately 0.35711 and 7.14217, respectively.

Proof. Note first that the inequality in (1) only apply to hyperbolic diagrams. So, if H is the event that the diagram is hyperbolic, then

$$\mathbb{E}[Vol_n] = \mathbb{E}[Vol_n | H]P(H) + 0$$

as the volume is 0 in the other case.

Which diagrams in this model are not hyperbolic? As mentioned before, due to [13], any such diagram must represent a torus link; however, there are just two such diagrams, the two rootings of the standard diagram of the 2-braid torus link $T(2, n)$ [19], as in Figure 4.3. For hyperbolic diagrams, we have the fact that the twist number t is the number of crossings n minus the number of bigons N_2 , so we can compute the expected twist number for hyperbolic diagrams. For the two exceptions of $T(2, n)$, we have n crossings, n bigons, and twist number 1. That is, the conditional expectation for N_2 is

$$\mathbb{E}[N_2] = \mathbb{E}[N_2 | H]P(H) + n(P(H^c))$$

In the hyperbolic case, we can compute the expected twist number using Theorem 4.5.

$$\begin{aligned} \mathbb{E}[t | H] &= n - \mathbb{E}[N_2 | H] \\ &= n - (\mathbb{E}[N_2] - nP(H^c))\frac{1}{P(H)} \\ &= n - (2nP(2, n) + O(na^n) - nP(H^c))\frac{1}{P(H)} \\ &= n - \left(2n\left(\frac{4}{27} + \frac{10}{27n} + O\left(\frac{1}{n^2}\right)\right) + O(na^n) - nP(H^c)\right)\frac{1}{P(H)} \end{aligned}$$

Expanding out everything, and combining the asymptotically small terms gives

$$\begin{aligned}
&= \left(nP(H) - \frac{8n}{27} + \frac{20}{27} + O\left(\frac{1}{n}\right) \right) \frac{1}{P(H)} \\
&= \left(n(1 - P(H^c)) - \frac{8n}{27} + \frac{20}{27} + O\left(\frac{1}{n}\right) \right) \frac{1}{P(H)} \\
&= \left(\frac{19n}{27} - nP(H^c) + \frac{20}{27} + O\left(\frac{1}{n}\right) \right) \frac{1}{P(H)}
\end{aligned}$$

Absorbing the exponentially small term $nP(H^c)$ into $O(\frac{1}{n})$, we get

$$= \left(\frac{19n}{27} + \frac{20}{27} + O\left(\frac{1}{n}\right) \right) \frac{1}{P(H)}$$

With this, we are finally set up to bound the expected volume. For hyperbolic diagrams, we have by linearity and monotonicity of expectation, as well as (1)

$$\begin{aligned}
\frac{v_3}{2}(t-2) &\leq Vol_n < 10v_3(t-1) \\
\frac{v_3}{2}(\mathbb{E}[t \mid H] - 2) &\leq \mathbb{E}[Vol_n \mid H] < 10v_3(\mathbb{E}[t \mid H] - 1)
\end{aligned}$$

Multiplying through by $P(H)$, we get the expected volume over all diagrams, and with the result of the computation of the expected twist number, we get

$$\begin{aligned}
\frac{v_3}{2} \left(\frac{19n}{27} + \frac{20}{27} + O\left(\frac{1}{n}\right) - 2P(H) \right) &\leq \mathbb{E}[Vol_n] < 10v_3 \left(\frac{19n}{27} + \frac{20}{27} + O\left(\frac{1}{n}\right) - P(H) \right) \\
\frac{19v_3}{54}n + \frac{10v_3}{27} - 2 + O\left(\frac{1}{n}\right) &\leq \mathbb{E}[Vol_n] < \frac{190v_3}{27}n + \frac{200v_3}{27} - 1 + O\left(\frac{1}{n}\right)
\end{aligned}$$

Again, we have replaced the $P(H)$ terms with $1 - P(H^c)$ and absorbed those exponentially small terms into the $O(1/n)$. So, the result is obtained. □

So, the expected volume is bounded below and above by linear functions, up to some terms that go to zero for large n . The upper bound we get from this process is worse than the bound we would have gotten from using the octahedral bound. For an n crossing link diagram representing a link K , this bound gives that

$$Vol(S^3 - K) \leq v_8 n$$

This bound applies for the nonhyperbolic cases trivially, so by taking expectation, we get the following bound.

Lemma 4.7. *The expected hyperbolic volume Vol_n of a random alternating link diagram with n crossings is bounded above:*

$$\mathbb{E}[Vol_n] \leq v_8 n \quad (4)$$

where $v_8 \approx 3.6638$ is the volume of a regular hyperbolic ideal octahedron.

Hence, for a slightly stronger result, we can use the lower bound from the proof above and the upper bound from the octahedral decomposition, giving the statement of Theorem 1.1 in the introduction.

Theorem 1.1 (Improved). *The expected hyperbolic volume $\mathbb{E}[Vol_n]$ of an n -crossing alternating link diagram is bounded by*

$$\left(\frac{19v_3}{54}\right)n + \left(\frac{10v_3}{27} - 2\right) + O\left(\frac{1}{n}\right) \leq \mathbb{E}[Vol_n] \leq v_8 n$$

Numerically, the coefficients on n of the lower bound and upper bounds are approximately 0.3571 and 3.6638, respectively.

We'd like to divide by n and take a limit, but it's unknown whether the expected volume per crossing converges to any limiting value. Accordingly, we offer this seemingly intractable question as a conjecture. We also present experimental evidence for it in the next section.

Conjecture 4.8. *The expectation of the hyperbolic volume per crossing,*

$$\frac{1}{n}\mathbb{E}[Vol_n]$$

converges to a limiting value as $n \rightarrow \infty$.

However, we can still state limiting behavior in terms of \liminf and \limsup .

Corollary 4.9. *Let Vol_n be the random variable which returns the hyperbolic volume of a random alternating link diagram with n crossings. The expected hyperbolic volume per crossing is bounded by*

$$\frac{19v_3}{54} \leq \liminf_{n \rightarrow \infty} \left(\frac{1}{n}\mathbb{E}[Vol_n]\right) \leq \limsup_{n \rightarrow \infty} \left(\frac{1}{n}\mathbb{E}[Vol_n]\right) \leq v_8$$

The conjecture then would be that the \liminf and \limsup above are actually equal.

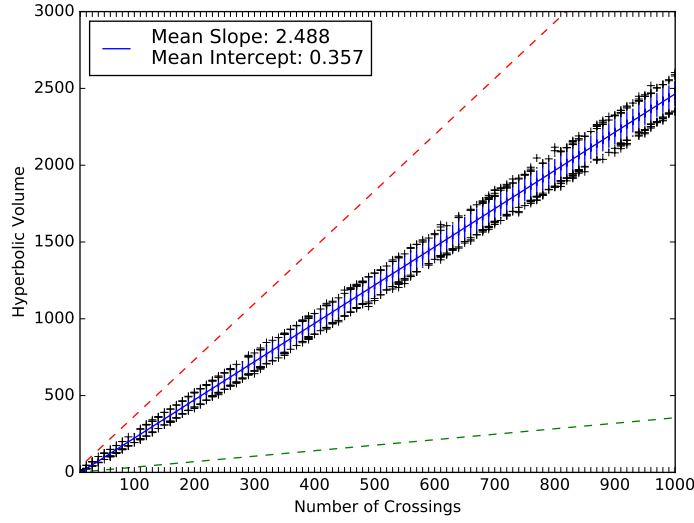


Figure 4.4: Box-and-whisker plot of volumes of alternating links for a range of sizes. We generated 10,000 samples of size 10, 20, 30, etc. up to 1000. The dashed lines are the bounds from Theorem 1.1, and the plus signs are outliers.

4.2 Numerical Experiments

The random link sampling algorithm is incorporated into SnapPy; we can look at the distribution of volumes that we get for different sizes of alternating diagrams. Here we generated 1 million random diagrams of varying sizes, ranging from 10 to 1000 crossings, every 10 crossings, and plot in Figure 4.4.

The volume does in fact appear to grow linearly, with slope around 2.5, which is then the observed expected volume per crossing. The variances are plotted in Figure 4.5, and appear to grow linearly as well. We can also look at the distribution for a given number of crossings, which we plot in Figure 4.6.

Experimentally, the distributions skew slightly to the left. For each number of crossings, we took a million samples of volumes of random alternating link diagrams and computed the skew, which appears to be consistently small but negative. A possible explanation for this is that the distribution for the number of bigons (when normalized) appears to be slightly skewed in the other direction, positively (Figure 4.8).

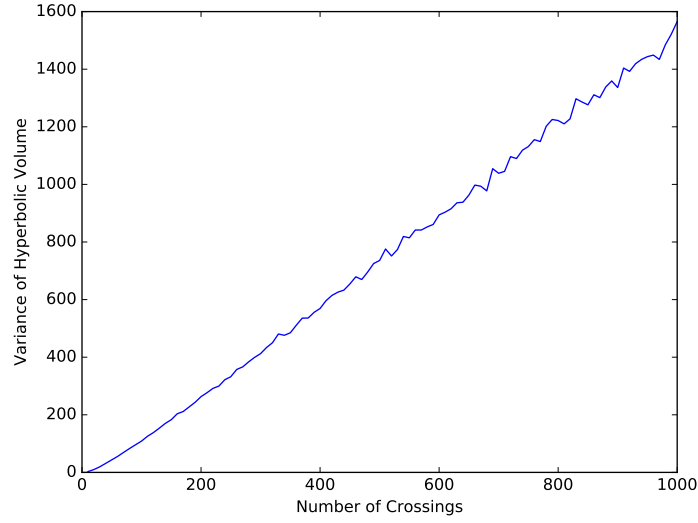


Figure 4.5: Plot showing the growth of the variance of the data in Figure 4.4.

Number of Crossings	Skewness of Volume	Skewness of Number of Bigons
100	-0.093858033849	0.040877113357
300	-0.049351483215	0.018498451862
500	-0.048770255118	0.018192743976
700	-0.050229963233	0.014187648283
900	-0.052681105543	0.011986807300
1100	-0.051342016899	0.015350076951

In fact, we can look at some higher moments as well (see Figure 4.7) and note that those also appear to vaguely tend towards limiting values, though the data is sparser than the above. This could lead one to conjecture the following.

Conjecture 4.10. *The normalized distribution of Vol_n in this model converges to a skewed limiting distribution as $n \rightarrow \infty$.*

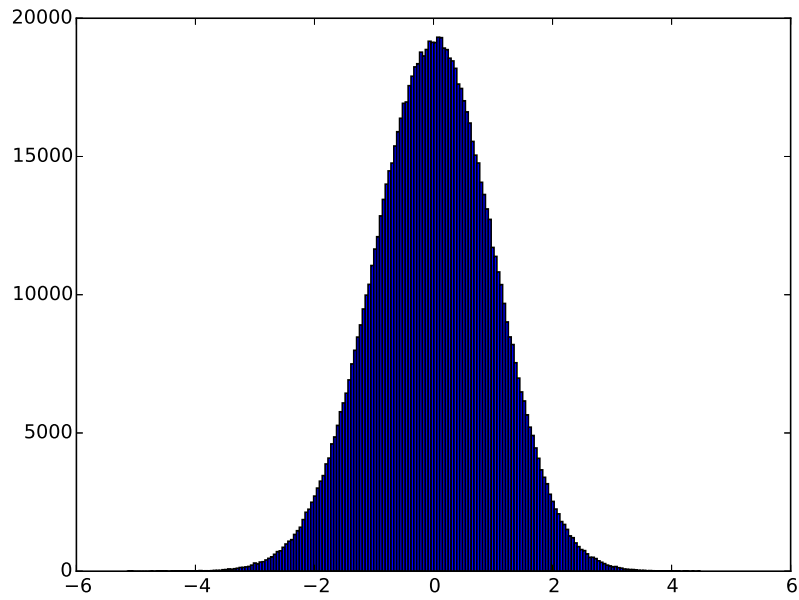


Figure 4.6: Histogram for the volumes of 1 million randomly sampled alternating links with 900 crossings, normalized to mean 0 and variance 1. The actual mean and variance were approximately 2216.46 and 1371.02 respectively.

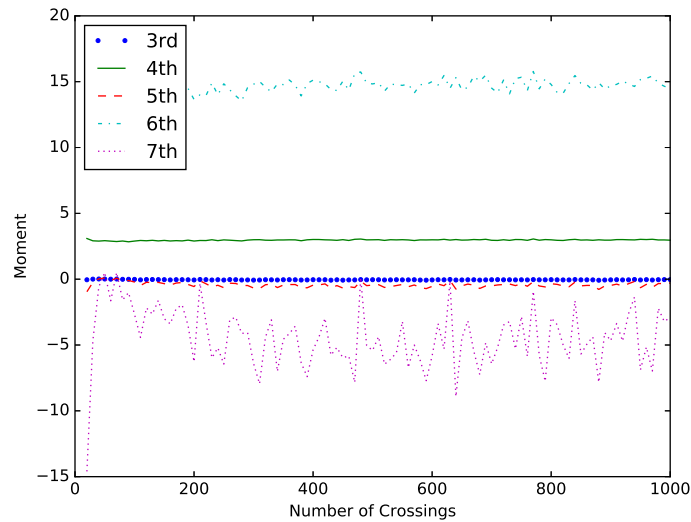


Figure 4.7: Some higher moments for alternating link diagrams sampled from crossing number 20 to 1000.

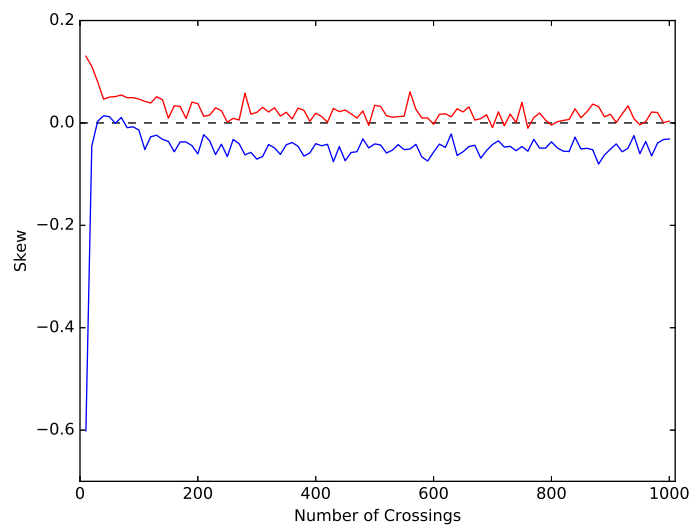


Figure 4.8: The skews for the volume and number of bigons for collections of samples ranging from 10 crossings to 1000. The skew for the volume (the lower graph) tends to be slightly negative, and for the number of bigons (the upper graph) slightly positive.

CHAPTER 5

Coin Flip Diagrams

In Chapter 3, we defined what is meant by a tangle T embedding within a link diagram: the existence of an embedded circle in S^2 intersecting along some number of edges so that cutting along this circle gives T . Such a circle is more naturally thought of as being a *cycle in the dual planar map*.

Recall that the *face* of a planar map D is one of connected components $S^2 \setminus D$; topologically, these are all disks. The *size* of a face F is the number of edges touching F , where edges that have F on both sides are counted twice. See Figure 5.1 for an example, and [15] for a more detailed exposition.

The *dual* D^* of a planar map D is defined by placing one vertex in the center of each face of D , and for each edge $e \in D$, there is a corresponding edge $e^* \in D^*$ crossing e and connecting the vertices corresponding to the faces on each side of e . We can also make a convention to transfer the root to the dual — edge r^* in D^* is the root edge, oriented so that its root vertex is the root face of D . That is to say, from the perspective of the root of D , the edge in D^* crossing right to left is the root of D^* . Note that by this convention, taking

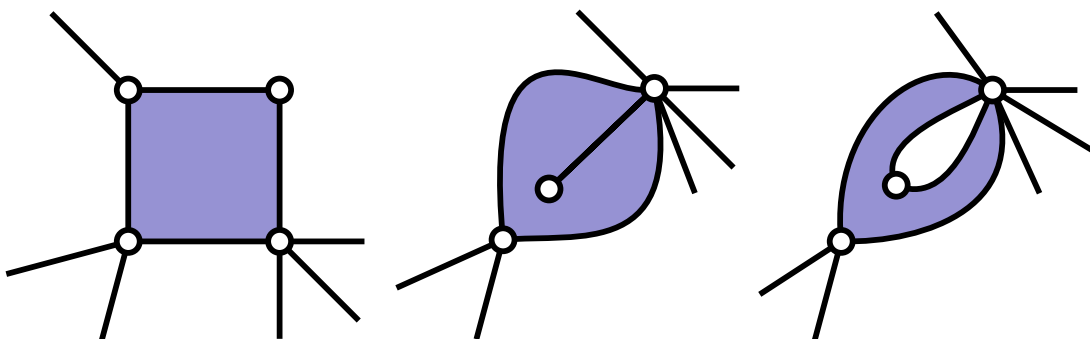


Figure 5.1: The shaded face above in each diagram has size 4. The middle diagram is obtained by gluing two edges in the leftmost diagram. The rightmost diagram is obtained by gluing two vertices in the leftmost diagram.

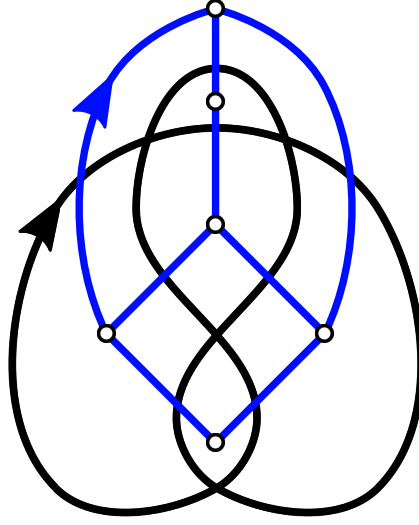


Figure 5.2: The dual of a planar map.

the dual twice actually flips the orientation of D , but this will not be relevant in any of our arguments.

Dual to a four valent planar map is a map where all faces have size four. Such a map is called a *quadrangulation*. However, as some of the faces around a crossing can actually be the same face (for example, if there is a loop at the vertex), some of the edges or vertices can be glued together. We denote the set of all quadrangulations with n faces by $Q^1(n)$; note that the dual map described above is a bijection between $Q(n)$ and $Q^1(n)$.

In this dual picture, a connected tangle shadow is dual to a *quadrangulation with simple boundary*. A *quadrangulation with simple boundary* is defined as a planar map where all faces have size 4, except for one face (called the *exterior face*), which has arbitrary even size, and which has each vertex occurring exactly once when walking around the boundary.

We denote by $Q^1(n, p)$ the set of all quadrangulations with simple boundary with n non-exterior faces and $2p$ boundary vertices, and rooted so that the root face is the exterior face. In other words, so that the face to the right of the root is the exterior face. A quadrangulation with boundary will typically be drawn so that its exterior face contains the point at infinity, so that the root is oriented counterclockwise around the boundary. See Figure 5.3.

An *cycle of length $2p$* in a quadrangulation is a sequence of oriented edges $(e_1, e_2, \dots, e_{2p})$ so that the end vertex of e_i coincides with the start vertex of e_{i+1} for $i \in \{1, 2, \dots, 2p\}$. Here, e_{2p+1} is taken to be e_1 , so that the cycle ends where it began. Note that in a quadrangulation, cycles of odd length are impossible, as quadrangulations are two-colorable.

A cycle $(e_1, e_2, \dots, e_{2p})$ is *embedded* if in the sequence of starting vertices $(v_1, v_2, \dots, v_{2p})$ of

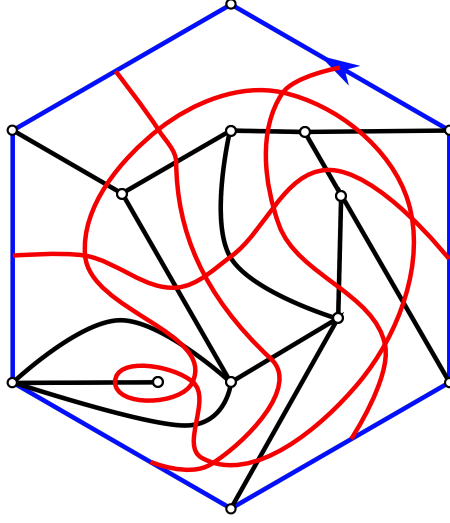


Figure 5.3: A quadrangulation with simple boundary, and the dual tangle shadow.

the edges $(e_1, e_2, \dots, e_{2p})$, no vertex v_i occurs more than once.

In [5], there is a “global” count of how many times a given tangle occurs in a diagram. To get a quantitative “local” version, we will use the root as a reference point in the diagram, and compute the probability that a given tangle occurs “at the root”. With this in mind, we will refer to an element of $Q^1(n, p)$ as a *local picture*.

If there is an embedded cycle c of oriented edges, of length $2p$, going through the root of a quadrangulation $D \in Q^1(N)$, it splits D into $D_c \in Q^1(n_c, p)$ on the side *left* of the cycle, and another quadrangulation with boundary on the right side, but where the root is in the opposite direction of the convention above in the definition of $Q^1(n, p)$.

Given a local picture $T \in Q^1(n, p)$ and a quadrangulation $D \in Q^1(N)$, we say that T *embeds around the root* if there is an embedded cycle c of length $2p$ in D so that D_c is rooted equivalent to T .

Proposition 5.1. *If T embeds around the root of $D \in Q^1(N)$, it does so uniquely. In other words, there is at most one simple cycle going through the root in D , where D_c is equivalent to T .*

Proof. The cycle in D corresponding to the boundary cycle of T , if it exists, must cross the same number of edges *to the left side* as the boundary cycle in T . So, because the boundary of T is simple, we can obtain a list of instructions for how to walk around the corresponding

cycle in D . Start by walking along the roots of D and T in the direction of the roots; at each vertex, go along the k -th edge *clockwise* from the previous edge, where $k + 1$ is the valence of the vertex in T , so that we are still going along the boundary face of T . Therefore, the cycle in D is determined from just T , and D_c is uniquely determined from T . \square

Enumerations of $Q^1(n, p)$ were computed by Bouttier and Guitter in [21]. In fact, these enumerations are enough to compute the probability that a given $T \in Q^1(n, p)$ occurs around the root of a random element of $Q^1(N)$, which would let us find the probability that a given tangle diagram occurs around a specific edge. However, if we want to compute the *number* of times a given T occurs, we need more information. So, we will generalize to allow multiple simple boundary components, as follows.

For any quadrangulation D , define an r -*multirooting* to be an ordered list of r distinct oriented edges in D . By “distinct oriented edges”, we are allowing an oriented edge its reverse to be considered distinct. We call two multirooted quadrangulations D_1 and D_2 *multirooted equivalent* if there is an orientation preserving homeomorphism of the sphere which sends D_1 to D_2 as maps, and which send the i -th root of D_1 to the i -th root of D_2 for all $1 \leq i \leq r$.

We denote by $Q^r(N)$ the set of all r -multirooted quadrangulations with N faces, considered up to multirooted equivalence. We will also refer to the set of *unrooted* planar quadrangulations with N faces, which we call $Q^0(N)$.

First, we consider the effect of adding another root. Define a *forgetful map* $f_r : Q^{r+1}(N) \rightarrow Q^r(N)$ which keeps the same quadrangulation but forgets the final oriented edge in the multirooting.

Lemma 5.2. *The map $f_0 : Q^1(N) \rightarrow Q^0(N)$ is $4N$ -to-1, except for an exponentially small number of elements of $Q^0(N)$. That is, for a random D in $Q^0(N)$,*

$$\Pr [|f_1^{-1}(D)| \neq 4N] = O(a^{-N})$$

for some constant $a > 1$.

For $r \geq 1$, $f_r : Q^r(N) \rightarrow Q^{r-1}(N)$ is exactly $(4N - r)$ -to-1.

Proof. The first part of the lemma is a result of Richmond and Wormald [18].

For $r \geq 1$ and $D \in Q^r(N)$, there are $4N - r$ elements of $Q^{r+1}(N)$ which are sent to D by f_r : there are $4N - r$ choices left for the final root from the set of all $4N$ oriented edges, disallowing any of the r roots already present. Two different choices of oriented edge cannot result in the same diagram; any equivalence must already fix the first root, and the rest of the map is automatically determined from this. \square

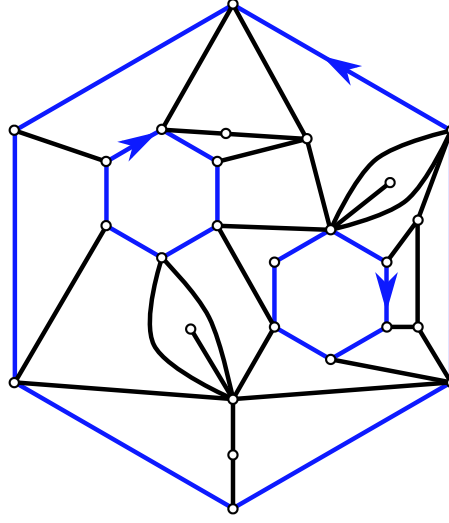


Figure 5.4: A quadrangulation with 3 simple, disjoint boundaries of length 6 and 16 non-exterior faces, i.e. an element of $Q^3(16, 3)$.

An r -multirooted quadrangulation with simple boundaries of length $2p$ is a planar map D with the following properties:

- (I) All faces of D have size 4, except for r faces which have size $2p$, called the *exterior faces*.
- (II) The map is r -multirooted, with each root having one of the exterior faces on its right side (as its root face), and where no two roots share the same root face.
- (III) The boundary cycles of the exterior faces are disjoint.

Denote the set of all r -multirooted quadrangulations with N *non-exterior* faces and r boundaries of length $2p$ by $Q^r(N, p)$. That is to say, an element of $Q^r(N, p)$ has N quadrilateral faces and r faces of size $2p$, for a total of $N + r$ faces. There is an enumeration of $Q^r(N, p)$ due to Bernardi and Fusy [22]. We will only need the asymptotic behavior for large N , which we compute here:

Lemma 5.3. *The number of r -multirooted quadrangulations with simple boundaries of length*

p and N faces is

$$|Q^r(N, p)| \approx \frac{\left(2^{p+1}3^{-p}p\binom{3p}{p}\right)^r}{2\sqrt{\pi}}12^N N^{r-3-1/2}(1 + O(1/N))$$

Proof. The enumeration in [22] is in terms of the number of internal vertices m . We will compute asymptotics of this expression for large m , and then convert to the number of faces N at the end.

According to Theorem 1.2 in [22], the number of multirooted maps with m internal vertices, r simple boundaries, with roots along the boundary faces, is, in their notation, given by

$$|Q[m; 2p, 2p, \dots, 2p]| = \frac{3^k(e-1)!}{m!(3b+k)!} \left(2p\binom{3p}{p}\right)^r$$

Here, $b := rp$ is half the total boundary length, $k := r + m - 2$, and $e = 3b + 2k$ is the number of edges. Substituting everything in terms of m , r , and p , and grouping all terms which are constant in m into a term C , we get:

$$|Q[m; 2p, 2p, \dots, 2p]| = C \left(\frac{3^m(2m + 3rp + 2r - 5)!}{m!(m + 3rp + r - 2)!} \right)$$

where $C := 3^{r-2} \left(2p\binom{3p}{p}\right)^r$

We use Stirling's approximation $n! \approx \sqrt{2\pi}e^{-n}n^{n+1/2}(1 + O(1/n))$ on each of the factorial terms to approximate for large m . To simplify the notation, we will group the expression into the terms which are constant in m , called C' , the terms which are polynomial in m , P , the terms which have m in the exponent, E .

$$|Q[m; 2p, \dots, 2p]| \approx (C)(P)(E)(1 + O(1/m))$$

$$\begin{aligned} \text{where } C' &:= \frac{C}{\sqrt{2\pi}e^{r-3}} = \frac{3^{r-2} \left(2p \binom{3p}{p}\right)^r}{\sqrt{2\pi}e^{r-3}} \\ P &:= \frac{(2m + 3rp + 2r - 5)^{3rp+2r-5+1/2}}{m^{1/2}(m + 3rp + r - 2)^{3rp+r-2+1/2}} \\ E &:= (3^m) \frac{(2m + 3rp + 2r - 5)^{2m}}{m^m(m + 3rp + r - 2)^m} \end{aligned}$$

We rewrite E using polynomial long division as follows:

$$\begin{aligned} E &= (3^m) \left(\frac{(2m + 3rp + 2r - 5)^2}{m^2 + (3rp + r - 2)m} \right)^m \\ &= (3^m) \left(4 + \frac{4m(r - 3) + (3rp + 2r - 5)^2}{m^2 + (3rp + r - 2)m} \right)^m \\ &= (12^m) \left(1 + \frac{m(r - 3) + (3rp + 2r - 5)^2}{m^2 + (3rp + r - 2)m} \right)^m \\ &= (12^m) \left(1 + \frac{(r - 3)}{m + 3rp + r - 2} + \frac{(3rp + 2r - 5)^2}{m^2 + (3rp + r - 2)m} \right)^m \end{aligned}$$

Up to a term that can be absorbed into the final $1 + O(1/m)$, the penultimate term is approximately e^{r-3} . We can see this by noting that

$$\left(1 + \frac{A}{m} + \frac{B}{m^2} \right)^m = e^A(1 + O(1/m))$$

This is done by taking logs, and expanding the power series. Collecting together all the terms from C' , P , and E , we get a final asymptotic approximation:

$$|Q[m; 2p, \dots, 2p]| \approx \frac{2^{3rp+3r-5} p^r \binom{3p}{p}^r 3^{r-2}}{\sqrt{\pi}} 12^m m^{r-3-1/2} (1 + O(1/m))$$

By an Euler characteristic argument, we can rewrite this instead using the number of faces:

$$m = N + 2 - (p + 1)r$$

Therefore,

$$|Q^r(N, p)| \approx \frac{2^{3rp+3r-5} p^r \binom{3p}{p}^r 3^{r-2} 12^{2-(p+1)r}}{\sqrt{\pi}} 12^N N^{r-3-1/2} (1 + O(1/N))$$

After collecting together powers of 2, 3, and 12, we get the formula in the statement of the lemma. □

We wish to find the probability of a tangle occuring in a part of a diagram. A connected tangle with n crossings and $2p$ points on the boundary is dual to quadrangulation with 1 simple boundary, with n faces, and boundary length $2p$. Fixing a root along the boundary gives an element of $Q^1(n, p)$. We will call an element of $Q^1(n, p)$ a *local picture*.

Given a T , we define an indicator random variable Emb_i^T on $Q^r(N)$, with the uniform probability measure. So, $Emb_i^T(D) = 1$ exactly when T embeds around the i -th root of D . Note that $\mathbb{E}[Emb_i^T]$ is the probability that T embeds around the i -th root in a random r -multirooted diagram.

We want to show that T has a positive probability of embedding around each of the roots, and that for very large diagrams, the behavior around each of the roots is essentially uncorrelated. First, we show that the probability that the roots are close to each other is small.

We call the *face distance* $d_{face}(F_1, F_2)$ between two faces F_1 and F_2 in a quadrangulation D the minimal number of edges of D a path from the interior of F_1 to the interior of F_2 must cross (without crossing vertices). Note that this is just the graph metric on the dual graph.

For an oriented edge e , denote the face to the right side of e by $f(e)$.

Lemma 5.4. *Fix a constant C . For a random element $D \in Q^r(N)$, with roots (e_1, e_2, \dots, e_r) . Then,*

$$\Pr [d_{face}(f(e_i), f(e_j)) < C \text{ for any } i \neq j] = O(\frac{1}{N})$$

Proof. By Lemma 5.2, only an exponentially small portion of quadrangulations have auto-

morphisms, so an element of $Q^r(N)$ can be specified by starting with an unrooted quadrangulation, and then choosing a sequence of r distinct, oriented edges, one at a time. That is, an exponentially small fraction of $Q^0(N)$, the set of unrooted quadrangulations with N faces, the total number of ways to do this is

$$(4N)(4N - 1)\dots(4N - r)$$

We can enumerate elements of $Q^r(N)$ whose roots are far apart using this choice, as follows: first, take one of the $4N$ choices of oriented edge to be e_1 . Next, choose any of the oriented edges whose faces do not lie inside the ball of radius $C + 2$ of the face of e_1 . This forces $d_{face}(f(e_1), f(e_2))$ to be at least C . There are at most a bounded number of elements (bounded in N) in the ball for fixed C . Each face borders at most 4 others, so in the worst case, there are at most $1 + 4 + 4^2 + \dots + 4^{C+2} = (4^{C+3} - 1)/3$ elements in the ball of radius $C + 2$ around a face. There are at most four times as many edges whose corresponding faces lie in this ball, giving a fixed upper bound $B = 4(4^{C+3} - 1)/3$ on the number of oriented edges within distance C of e_1 . This means that there are at least $4N - B$ choices for oriented edges at distance at least C from e_1 . For e_3 , we make a choice among all the edges at least distance C from both e_1 and e_2 , and continue as such, giving

$$(4N)(4N - B)(4N - 2B)\dots(4N - rB)$$

choices for the roots, where all roots are at least distance C from all other roots. So, as a probability,

$$\begin{aligned} \Pr [d_{face}(f(e_i), f(e_j)) > C \text{ for some } i \neq j] &> \frac{(4N)(4N - B)(4N - 2B)\dots(4N - rB)}{(4N)(4N - 1)(4N - 2)\dots(4N - r)} \\ &= 1 - O\left(\frac{1}{N}\right) \end{aligned}$$

□

We want to compute the probability that a given local picture $T \in Q^1(n, p)$ occurs around all r roots of an element of $Q^r(N)$. In the end, we will need only the cases $r = 1$ (to compute the expectation of Emb_i^T) and $r = 2$ (to compute covariance between Emb_i^T and Emb_j^T) to show that a generic link diagram is composite.

Proposition 5.5. *The probability that $T \in Q^1(n, p)$ embeds around all roots in a random*

element $D \in Q^r(N)$ is given by

$$\mathbb{E}[Emb_1^T Emb_2^T \dots Emb_r^T] = (P_{lim}(n, p))^r + O(\frac{1}{N})$$

where

$$P_{lim}(n, p) = \frac{3 \cdot 2^{(3p+1)} p \binom{3p}{p}}{12^{(p+1+n)}}$$

Proof. We want to count the number of maps $D \in Q^r(N)$ where T embeds around each of the root edges (e_1, e_2, \dots, e_r) . Suppose that T has n faces and $2p$ boundary vertices. We can count these maps as follows. Suppose that T embeds around all e_i . Then, deleting each of those r copies of T yields a quadrangulation with r boundary components, assuming that those copies of T do not intersect with one another. However, by Lemma 5.4, the probability that the roots are near enough for copies of T to intersect goes to zero as the size of the diagram grows. We can write the expectation in the statement of the proposition above as follows, by the law of total expectation:

$$\begin{aligned} \mathbb{E}[Emb_1^T Emb_2^T \dots Emb_r^T] &= \Pr[T \text{ embeds around all roots without intersection}] \\ &\quad + \Pr[T \text{ embeds around all roots with intersection}] \end{aligned}$$

The second term is $O(1/N)$ by Lemma 5.4, as any such intersection would require that the roots be near each other.

So, we can just focus on computing the probability that T embeds around each root without intersection. Deleting the each of these copies of T results in an element of $Q^r(N - rn, p)$. In fact, this map is a bijection; we can define an inverse map by gluing r copies of T to an element of $Q^r(N - rn, p)$ so that the roots line up. So, we can use our previous computation of the asymptotics of $|Q^n(N, p)|$, with a single substitution.

$$|Q^r(N - rn, p)| \approx \frac{\left(2^{p+1} 3^{-p} p \binom{3p}{p}\right)^r}{2\sqrt{\pi}} 12^{N-rn} (N - rn)^{r-3-1/2} (1 + O(1/N))$$

The above expression is then, asymptotically, the number of elements in $Q^r(N)$ for which T embeds around each root. To compute the probability, we also find an asymptotic expression for $|Q^r(N)|$ and divide. Recall that, as shown in the proof of Lemma 5.4, we can enumerate all elements of $Q^r(N)$ by picking an element of $Q^1(N)$ and choosing $r - 1$ more oriented edges. The number of elements in $Q^1(N)$ was enumerated by Tutte [15]; we use Stirling's

approximation again to get an asymptotic formula:

$$\begin{aligned}
|Q^r(N)| &= |Q(N)|(4N)(4N-1)(4N-2)\dots(4N-(r-1)) \\
&= \left(\frac{2(3^n)(2n)!}{n!(n+2)!} \right) (4N)(4N-1)\dots(4N-(r-1)) \\
&\approx \frac{2}{\sqrt{\pi}} 12^N (N+2)^{-5/2} (4N)(4N-1)(4N-2)\dots(4N-(r-1)) (1 + O(1/N)) \\
&= \frac{2}{\sqrt{\pi}} 12^N (N+2)^{-5/2} (4^{r-1})(N)(N-\frac{1}{4})(N-\frac{2}{4})\dots(N-\frac{r-1}{4}) (1 + O(1/N))
\end{aligned}$$

Note that for the polynomial parts of both $|Q^r(N)|$ and $|Q^r(N-rn, p)|$, the leading power of N in each case is $N^{r-7/2}$, and for the exponential parts, both grow like 12^N . Dividing and simplifying, this coincidence gives a limiting probability that T embeds around all roots that is bounded away from zero:

$$\frac{|Q^r(N-rn, p)|}{|Q^r(N)|} \approx \left(\frac{3 \cdot 2^{(3p+1)} p \binom{3p}{p}}{12^{(p+n+1)}} \right)^r (1 + O(1/N))$$

We call the term

$$P_{lim}(n, p) = \frac{3 \cdot 2^{(3p+1)} p \binom{3p}{p}}{12^{(p+n+1)}}$$

completing the proof of the proposition. \square

We only need the $r = 1$ and $r = 2$ cases of Proposition 5.5 in order to show that a generic link diagram is composite. The $r = 1$ case corresponds to the probability for a random diagram in $Q(N)$ that a given local picture T embeds around the root edge. In that case, we get the following corollary:

Corollary 5.6.

$$\mathbb{E}[Emb_1^T] = (P_{lim}(n, p))(1 + O(1/N))$$

Know that the expectation of the number of times T occurs is growing, does *not* mean that with probability tending to 1, that T must occur; it only guarantees that it must occur for a subset of positive probability.

In order to make precise this counting of the number of times T embeds into a diagram, we need to add a small extra bit of structure. Instead of considering rooted or multirooted quadrangulations, we define a *labeling* for a quadrangulation with N faces to be an assignment of labels $(1, 2, \dots, 4N)$ to each oriented edge in the diagram. Then, we define $LQ(N)$

to be the set of quadrangulations with a fixed labeling, up to ambient isotopy which sends labels to corresponding labels. We could think of this as a multirooting where every oriented edge is a root; that is, $LQ(N)$ is essentially $Q^{4N}(N)$ in the previous notation.

Then, for a fixed local picture T , we define a function Num^T on $LQ(N)$ by

$$Num^T(L) = \# \text{ of oriented edges around which } T \text{ embeds}$$

Define an analogous function Emb_i^T as the indicator variable for whether T embeds around the oriented edge labeled i .

Then, as random variables on $LQ(N)$,

$$Num^T = \sum_{i=1}^{4N} Emb_i^T$$

The probability that T embeds around edge i is the same for a labeled diagram or a rooted diagram. This follows immediately from Lemma 5.2; the maps f_r are constant-to-one and do not affect the underlying maps at all. That is to say, the quantity computed in Proposition 5.5 is independent of whether the random variables Emb_i^T are considered as random variables on $Q^r(N)$, or on $Q^{r+1}(N)$, or by extension $Q^{4N}(N) = LQ(N)$. All oriented edges are equally likely to be edge i in each of the above (where $r \geq i$).

So, by linearity of expectation, we have the following

Corollary 5.7.

$$\mathbb{E}[Num^T] = \sum_{i=1}^{4N} \mathbb{E}[Emb_i^T] = P_{lim}(n, p)(4N)(1 + O(1/N))$$

In order to show that Num^T is generically positive, we need more information than just the expectation — we need to know something about the variance as well.

Lemma 5.8. *Consider the variance $Var[Num^T]$ of the random variable Num^T on $LQ(N)$. Then, the variance is bounded above by a linear function for large N . That is,*

$$Var[Num^T] = O(N)$$

Proof. The variance of the sum of indicator random variables can be bounded above by

$$Var[Num^T] < \mathbb{E}[Num^T] + \sum_{i \neq j} Cov[Emb_i^T, Emb_j^T]$$

The covariance terms are defined by

$$\text{Cov}[Emb_i^T, Emb_j^T] = \mathbb{E}[Emb_i^T Emb_j^T] - \mathbb{E}[Emb_i^T] \mathbb{E}[Emb_j^T]$$

The first term is the probability that T embeds at edges i and j , and the second is the product of the probabilities that it embeds at i and that it embeds at j . However, the probabilities above are exactly the same as those computed for the $r = 1$ and $r = 2$ cases of Proposition 5.5, because, for fixed i, j , the map

$$LQ(n) \rightarrow Q^1(N)$$

which forgets the labels and chooses edge i as the root, and the map

$$LQ(n) \rightarrow Q^2(N)$$

which forgets the labels and chooses edge i and j as the two roots, are both constant-to-one maps. That is, any edge is equally likely to be a root in $Q^r(N)$, and equally likely to be edge i in $LQ(N)$, so the probability that T embeds there is the same.

So,

$$\begin{aligned} \text{Cov}[Emb_i^T, Emb_j^T] &= \mathbb{E}[Emb_i^T Emb_j^T] - \mathbb{E}[Emb_i^T] \mathbb{E}[Emb_j^T] \\ &= (P_{lim}(n, p))^2(1 + O(1/N)) - P_{lim}(n, p)(1 + O(1/N))P_{lim}(n, p)(1 + O(1/N)) \\ &= O(1/N) \end{aligned}$$

Hence,

$$\begin{aligned} \text{Var}[Num^T] &< \mathbb{E}[Num^T] + \sum_{i \neq j} \text{Cov}[Emb_i^T, Emb_j^T] \\ &= O(N) + \sum_{i \neq j} O(1/N) \\ &= O(N) + N^2 O(1/N) \\ &= O(N) \end{aligned}$$

□

We now know the expectation $\mathbb{E}[Num^T]$ as well as the fact that variance $\text{Var}[Num^T]$ grows

at most linearly. The combination of these facts is enough to tell us, at least asymptotically, how many times we should expect a given tangle to appear in a random link diagram, as described in the following theorem.

Theorem 1.2. *Let T be an rooted, connected tangle diagram with n crossings and $2p$ boundary points, and let $Num^T(L)$ be the number of times T embeds in $L \in CF(N)$, a rooted link diagram with N crossings. Then,*

$$\mathbb{E}[Num^T] = \left(\frac{4P_{lim}(n, p)}{2^n} \right) N(1 + O(1/N))$$

where

$$P_{lim}(n, p) = \frac{3 \cdot 2^{(3p+1)} p^{\binom{3p}{p}}}{12^{(p+n+1)}}$$

Moreover, for any $\epsilon > 0$,

$$\Pr [Num^T < (1 - \epsilon)\mathbb{E}[Num^T] \text{ or } Num^T > (1 + \epsilon)\mathbb{E}[Num^T]] = O(1/N)$$

So, with high probability, Num^T is within any fixed fraction of its expectation for large N .

Proof. Each embedding of T into L corresponds to an embedding of the shadow of T into the shadow of L , so that all of the crossings also agree. The expected number of embeddings of T in L is exactly the same as the number of embeddings of the dual quadrangulation with boundary $T^* \in Q^1(n, p)$ into the dual quadrangulation $L^* \in Q^1(N)$. So, by the formula for the expectation in Corollary 5.7 gives us the expected number of embeddings, and since the crossings are independent coin flips, we simply divide by 2^n .

The second part follows from Chebyshev's inequality. Following [20], for any random variable X and $\lambda > 0$,

$$\Pr \left[|X - \mathbb{E}[X]| \geq \lambda \sqrt{Var[X]} \right] \leq \frac{1}{\lambda^2}$$

Choosing $\lambda = \epsilon \mathbb{E}[X] / \sqrt{Var[X]}$ gives

$$\Pr [|X - \mathbb{E}[X]| \geq \epsilon \mathbb{E}[X]] \leq \frac{Var[X]}{\epsilon^2 \mathbb{E}[X]^2}$$

For $X = Num^T$, we showed that $Var[Num^T] = O(N)$, so

$$\Pr [|Num^T - \mathbb{E}[Num^T]| \geq \epsilon \mathbb{E}[Num^T]] = \frac{O(N)}{\epsilon^2 O(N^2)} = O(1/N)$$

giving the second claim in the theorem. □

In the case that $p = 1$, Theorem 1.2 gives an explicit expression for how many times a given link diagram is an obvious connect summand in a random link diagram. This forces some invariants to grow linearly with high probability.

Corollary 5.9. *Let T be an rooted tangle diagram with n crossings and 2 boundary points, and let $X : CF(N) \rightarrow \mathbb{R}_{\geq 0}$ be any nonnegative link invariant which is additive under the connect sum. Denote by \overline{T} the link diagram obtained by connecting the 2 boundary points of T . Then,*

$$\mathbb{E}[X] \geq \frac{4X(\overline{T})}{24^n} N(1 - O(1/N))$$

Moreover, for any $\epsilon > 0$,

$$\Pr [X < (1 - \epsilon)4X(\overline{T})/24^n N] = O(1/N)$$

So, with high probability for large N , X is greater than a linearly function of N .

Proof. By additivity under connect sum and nonnegativity,

$$X(L) \geq \text{Num}^T(L) \cdot X(\overline{T})$$

where we have discarded the components which are not copies of T . Then, taking expectation, plugging $p = 1$ into the result of Theorem 1.2 above to evaluate $\mathbb{E}[\text{Num}^T]$ gives the desired expression for the expectation of X .

This same inequality of X immediately gives the result for the probability of X being small. □

Using, for example, the tangle obtained by cutting the figure 8 knot along one edge in Corollary 5.9 above, we can obtain lower bounds for certain invariants that are true with high probability for large N . For example, though the links in $CF(N)$ are generically composite, hence not hyperbolic, one can define an invariant, called the *Gromov invariant* G , which essentially extends the hyperbolic volume [27]. For a hyperbolic link L , $G(L) = \text{Vol}(L)/v_3$, so G is proportional to the hyperbolic volume. The invariant G is defined for any link, however, and satisfies

$$G(L_1 \# L_2) = G(L_1) + G(L_2)$$

i.e., G is additive under connect sum.

We also consider two other invariants, the *determinant* and the *Jones polynomial*. The get additive invariants, we consider the log of the determinant; the determinant itself is multiplicative under connect sum, so applying a logarithm gives an additive invariant. The Jones polynomial is also multiplicative under connect sum, so we instead consider the *breadth* b_J , which is the difference between the highest exponent and lowest exponent in Jones polynomial, which is well defined for unoriented link diagrams, and additive under the connect sum.

Corollary 1.3. *For a random link diagram in $CF(N)$, we have the following.*

- (I) *The Gromov invariant G : $\Pr[G < .000024N] = O(1/N)$*
- (II) *The log of the determinant $\log \det$: $\Pr[\log \det < .0003N] = O(1/N)$*
- (III) *The breadth of the Jones polynomial b_J : $\Pr[b_J < .0008N] = O(1/N)$*

Proof. For the Gromov invariant, we use a figure 8 knot, cut once to obtain a 2-tangle, which has $n = 4$ crossings, and has Gromov invariant 2. Computing the relevant coefficient in Corollary 5.9, and rounding down gives the desired result.

Similarly, for the log of the determinant, we use a trefoil, which has $n = 3$ crossings and $\log \det = \log 3$.

Finally, for the breadth of the Jones polynomial, we also use a trefoil, which has $b_J = 3$. \square

References

- [1] C. Even-Zohar, J. Hass, N. Linial, T. Nowik. Invariants of Random Knots and Links. <http://arxiv.org/pdf/1411.3308.pdf>
- [2] Y. Diao, N. Pippenger, D. W. Sumners On Random Knots. J. Knot Theory Ramifications 3. 1994.
- [3] J. Ma. The Closure of a Random Braid is a Hyperbolic Link. Proc. Amer. Math. Soc. 142, Number 2. 2014.
- [4] M. Cohen, S. Krishnan. Random knots using Chebyshev billiard table diagrams. <http://arxiv.org/abs/1505.07681>
- [5] H. Chapman. Asymptotic Laws for Knot Diagrams. <https://arxiv.org/pdf/1608.02638v1.pdf>
- [6] M. Lackenby. The volume of hyperbolic alternating link complements. Proceedings of the London Mathematical Society 88, Issue 1. 2004.
- [7] S. Garoufalidis, T. T. Q. Lê. Asymptotics of the colored Jones function of a knot. Geom. & Top 15. 2011.
- [8] D. Jungreis. Gaussian Random Polygons are Globally Knotted. J. Knot Theory Ramif. Vol 3, No 4. 1994.
- [9] M. Culler, N. M. Dunfield, M. Goerner, and J. R. Weeks. SnapPy, a computer program for studying the geometry and topology of 3-manifolds. <http://snappy.computop.org>
- [10] J. Hoste, M. Thistlethwaite, J. R. Weeks. The first 1,701,936 knots. The Mathematical Intelligencer 20 (4), 33-48. 1998.
- [11] G. Schaeffer. Bijective Census and Random Generation of Eulerian Planar Maps with Prescribed Vertex Degrees. Electron. J. Combin 4, Issue 1. 1997.
- [12] G. Schaeffer. *planarmap* Software. <http://www.lix.polytechnique.fr/~schaeffe/PagesWeb/PlanarMap/index-en.html>
- [13] W. Menasco. Closed incompressible surfaces in alternating knot and link complements. Topology 23. 1984
- [14] W. Tutte. A census of planar maps. Canad. J. Math. 1963.

- [15] W. Tutte. On the enumeration of planar maps. *Bull. Amer. Math. Soc.* 74. 1968.
- [16] W. Brown. Enumeration of non-separable planar maps. *Canad. J. Math.* 15. 1963.
- [17] B. Jacquard, G. Schaeffer. A Bijective Census of Nonseparable Planar Maps. *Journal of Combinatorial Theory, Series A* 83. 1998.
- [18] L. B. Richmond, N. C. Wormald. Almost All Maps Are Asymmetric. *Journal of Combinatorial Theory, Series B* 63. 1995.
- [19] C. Adams. Hyperbolic Knots. *Handbook of Knot Theory (Chapter 1)*. Elsevier Science. 2005.
- [20] N. Alon, J. Spencer. *The Probabilistic Method*. John Wiley & Sons. Third Edition, pp.47-48. 2004.
- [21] J. Bouttier, E. Guitter. Distance statistics in quadrangulations with a boundary, or with a self-avoiding loop. *Journal of Physics A: Mathematical and Theoretical* 42. 2009.
- [22] O. Bernardi, E. Fusy. Bijections for planar maps with boundaries. *Journal of Combinatorial theory, Ser. A*, 158, 176-227. 2018.
- [23] M. Krikun. Local structure of random quadrangulations. <http://arxiv.org/abs/math/0512304>
- [24] J. Hass. Algorithms for recognizing knots and 3-manifolds. *Chaos, Solitons & Fractals*, Vol. 9, No. 415, pp. 569-581. 1998.
- [25] J. R. Weeks. Computation of Hyperbolic Structures in Knot Theory. *Handbook of Knot Theory (Chapter 10)*. Elsevier Science. 2005.
- [26] R. Budney. JSJ-decompositions of knot and link complements in the 3-sphere. *L'enseignement Mathématique (2)* 52, pp. 319-359. 2006.
- [27] T. Soma. The Gromov Invariant of Links. *Invent. Math.* 64, pp. 445-454. 1981